

# HIGH-LATITUDE FJORD VALLEY FILLS: A CASE STUDY OF CLYDE FJORDHEAD, BAFFIN ISLAND, ARCTIC CANADA

IRINA OVEREEM

*Institute of Arctic and Alpine Research, University of Colorado, Boulder, Colorado 80303 USA*

*e-mail: irina.overeem@colorado.edu*

JASON P. BRINER

*Department of Geology, State University of New York, Buffalo, New York 14260 USA*

AND

ALBERT J. KETTNER, JAMES P.M. SYVITSKI

*Institute of Arctic and Alpine Research, University of Colorado, Boulder, Colorado 80303 USA*

**ABSTRACT:** Fjord valleys are carved during glaciation and then form local sediment sinks, which fill during retreat of the ice. Thus fjord valleys appear analogous to lower-latitude incised valleys, but they are remarkably different because fjords experience isostatic rebound during deglaciation, causing relative sea level to fall during infill.

This paper explores stratigraphic architecture of fjord valley fills based on Late Quaternary deposition in Clyde Inlet, Baffin Island, Arctic Canada, as constrained by 11 cosmogenic dates and 9 accelerator mass spectrometry (AMS)  $^{14}\text{C}$  datings.

A major ice stream of the Laurentide Ice Sheet occupied Clyde Inlet at last glacial maximum and bulldozed through a U-shaped valley forming a lower sequence boundary. During the Early Holocene the system entered a deglacial stage; tidewater glaciers retreated rapidly ( $>100$  km in 1000 yrs) through the fjord from 10.4 ka onward. Grounded ice lobes started retreating from the Clyde fjordhead by 9.4 ka. Then ice-contact fans (ICF) were deposited consisting of flat-topped fan deltas, covered with channels and boulder-strewn bars. Elevations of the surfaces vary between 62 and 77 m above sea level, which marks the relative sea level at the time of deposition and is considered to be the marine flooding surface. Marine muds have been draped directly onto the ICF complexes. Subsequently, coarse-grained glaciofluvial valley trains (GFVTs) prograde downstream caused by rapid base-level fall, despite possibly high sediment supply (i.e., forced regression). During the Late Holocene (3.5 ka) the last remaining lobes of the Laurentide Ice Sheet retreated from the middle parts of Clyde River basin to form the present Barnes Ice Cap. At this phase, the rate of base-level fall has decreased ( $\sim 1.6$  m/ka over the last 3.5 ka), still the river incises significantly, marking a reduced sediment supply. Narrow coarse sandy fluvial terraces were being deposited at the lowest level of the incised river valley. Clyde fjordhead may not have entered a postglacial stage by definition, nevertheless a strongly reduced sediment flux is apparent. Numerous upland lakes likely play a role in trapping sediment in the hinterland. In addition, we speculate that the glacial regime of the Barnes Ice Cap switched from a sediment producing regime to a nonerosive cold-based regime.

In conclusion, stratigraphic patterns of valley fills in high-latitude areas display an evident signature of isostatic rebound and a strongly varying sediment supply. Rapid uplift causes ice proximal units to occur high in the infill and reverses classic fining upward valley fill sedimentary trends. The exact interplay of local sea-level change and sediment supply dictates the complexity of the valley fill, but coarsening upward trends with younger sandy fluvial deposits incising into the fill deposits ultimately have important implications for the interpretation of similar deglacial valley fill settings.

**KEY WORDS:** glaciofluvial deposits, sequence stratigraphy, deglaciation, isostasy, sediment supply, forced regression

## INTRODUCTION

Fjord valleys carved in bedrock by ice streams over the Quaternary Period become important sediment sinks once the ice has retreated (Overeem and Syvitski 2010, Smith et al. 2015). At first appearance, such fjord valleys are analogous to incised river valleys on continental shelves, or to tunnel valleys near ice sheet margins (van der Vegt 2012). However, it has been noted that conceptual models for the infill of high-latitude valleys need to be critically different from the classical sequence stratigraphical model for incised valleys (Syvitski 1991, Powell and Cooper 2002, Corner 2006) for the following reasons:

1. Incised valleys on nonglaciated continental shelves are formed by river incision during sea-level fall and are infilled during subsequent sea-level rise (Dalrymple et al. 1994, 2007). In contrast, fjord valleys experience rapid isostatic rebound after deglaciation, which initially outpaces simultaneous global sea-level

rise causing sedimentary filling to occur under conditions of relative sea-level fall. Recent studies emphasize this “forced-regressive nature” of high-latitude valley fill deposits, which downstep basinward (Hansen 2004, Helle 2004, Eilertsen et al. 2007).

2. Sediment supply toward fjord valleys over time is more variable and complex than supply to lower-latitude incised valleys. Present-day glaciated basins worldwide have distinctly higher sediment yields than nonglaciated basins (Hallett et al. 1996). In Alaska, drainage basins with  $>30\%$  ice cover show order of magnitude higher sediment yields than nonglaciated basins (Guymon 1974). The volume of shelf deposits associated with the advance and retreat of Pleistocene ice sheets far exceeds extrapolated modern fluvial sediment delivery rates (Andrews 1987; Powell and Elverhoi 1989; Stravers and Syvitski 1991; Syvitski 1991; Syvitski and Hein 1991; Williams et al. 1995; Overeem et al. 2001, 2005). High sediment supply associated with glaciation prompts distinc-

Latitudinal Controls on Stratigraphic Models and Sedimentary Concepts

DOI: <https://doi.org/10.2110/sepmsp.108.05>

SEPM Special Publication No. 108, Copyright © 2019

SEPM (Society for Sedimentary Geology), ISBN 978-56576-346-3, eISBN 978-56576-347-0, p. 93–106.

tion between (1) the *deglacial stage of sedimentary valley infill*, when meltwater streams of retreating ice sheet tongues and local remnant glaciers are a major source of sediment, and (2) the *postglacial stage of valley fill*, when the catchment is ice free and local nonglacial rivers solely deliver sediment to the fjordhead (Corner 2006).

It must be noted, though, that the relation between glaciation of a basin and sediment yield is not entirely understood (Koppes and Montgomery 2009). Sediment yield shows intrinsic variability depending on glacial regime; whereas temperate valley glaciers are efficient erosive agents, polar glaciers are relatively modest sediment producers (Hallett et al. 1996). Another complicating factor is the concept of the paraglacial sediment cycle (Church and Slaymaker 1989, Ballantyne 2002), which predicts that high river sediment fluxes lag deglaciation. Sediment produced during active (de)glaciation is stored englacially initially and arrives at the margin with a delay (de Winter et al. 2012), and even when sediment is exposed it takes the fluvial system time to transport this pulse of sediment to the coast. The paraglacial sediment cycle model also implies that abrupt decoupling of a river basin from its ice sheet, and thus the transition from deglacial stage to postglacial stage, does not necessarily coincide with a drastic decrease of sediment supply rates. Here, we further investigate the timing of glaciation of a hinterland and its coherency with changes in basin sediment supply.

This paper aims to unravel the stratigraphic architecture of fjord valley fills based on detailed mapping of sedimentary deposits in Clyde Inlet, Baffin Island, Arctic Canada. The study area is well suited to disentangle the response of the sedimentary system to the main depositional controls, because climate, local deglaciation history, and associated sea level have been reconstructed in great detail (Dyke et al. 2002; Miller et al. 2002, 2005; Briner et al. 2005, 2006, 2007, 2008).

We consider Late Quaternary fjord valley systems as possible analogues for hydrocarbon-bearing ancient valley fill systems (e.g., Gondwana glaciations in Oman and Libya; de la Grandville 1982, Levell et al. 1988, Kalefa El-ghali 2005, Le Heron et al. 2006). Insight into the response of more recent fjord valley systems to variability of the main controls enhances the awareness of variability in the depositional architecture of ancient systems.

## GEOGRAPHIC SETTING

Baffin Island stretches over 1600 km and is the largest island in the Canadian Arctic (Fig. 1A). Northeastern Baffin Island consists of an interior plateau ~300–400 m above sea level (asl), and the high mountain range of the eastern Canadian Rim, which rises to ~1000–1500 m asl and is dissected by dozens of fjords (Fig. 1B).

This study focuses on Clyde River, located at 69°51' N and 70°27' W, which drains into Clyde Inlet, a 100-km-long fjord centrally located along the northeastern Baffin Island coast (Fig. 1B). The Clyde River drainage basin is 2526 km<sup>2</sup> (Canadian Topographic Survey Digital Elevation Model; Centre for Topographic Information 1998) and drains the southeasternmost part of the Barnes Ice Cap, a 150 by 400 km interior ice cap that is up to 650 m thick (Jacobs et al. 1993). The Barnes Ice Cap is a remnant of the Laurentide Ice Sheet (LIS) (Hooke 1976). The Clyde River originates in a large proglacial lake of the Barnes Ice Cap and flows 66 km across the interior plateau through a broad U-shaped valley containing numerous small lakes to the fjordhead of Clyde Inlet.

Basin mean annual temperature is –12.6° C, average monthly temperatures are above 0° C in June (1.0° C), July (5.0° C), August (4.3° C), and September (0.5° C), and mean annual precipitation is 220 mm (National Climate Data Centre, Clyde Airport Station

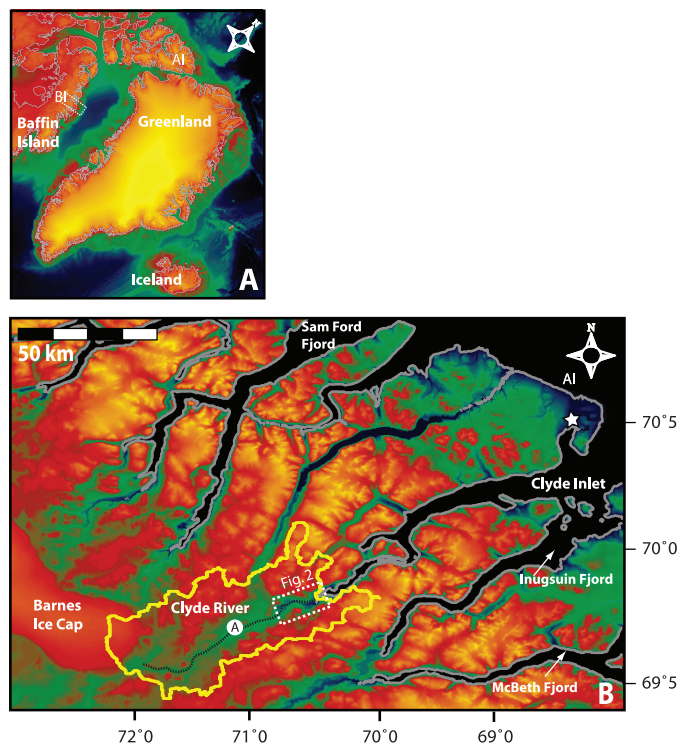


FIG. 1.—**A**) Topographic and bathymetric map of Baffin Island, Baffin Bay and Greenland based on the International Bathymetric Chart of the Arctic Ocean (IBCAO) Arctic Bathymetry dataset (WDC-MGG 2000) with Clyde Inlet region in Northeastern Baffin Island indicated by dotted line. AI indicates the Agassiz Ice Cap on Ellesmere Island, and BI indicated the Barnes Ice Cap on Baffin Island. **B**) Topographic map of Northeastern Baffin Island based on merged Digital Elevation Data of 1:250,000 mapsheets 037D, E, F, and 027F (Centre for Topographic Information 1998). Maps show the 120-km-long fjord of Clyde Inlet cutting through mountain range of the Canadian Rim. The drainage basin of Clyde River has been calculated from the digital elevation data and is indicated by the yellow line. The Barnes Ice Cap reaches up to 1000 m in the hinterland. Airport and meteorological station of Clyde River is indicated by a white star. Dotted line shows location of Clyde fjordhead as depicted in Figure 2. White circle A shows the location of bedrock samples in the middle reaches of Clyde River valley (Table 1).

701090), thus classifying Baffin Island as a polar desert (Thompson et al. 1999).

The Clyde River is not gauged, but the meteorological records as well as short-term gauging records of nearby river systems (Østrem et al. 1967, Church 1972) imply a 3 to 4 month discharge season and a limited snow-meltwater peak. The river remains frozen for the rest of the year.

The long and narrow fjord dampens wave action near the fjordhead, although locally small beach ridges point to some influence of waves on the coastal zone. Similarly, semidiurnal tides affect the fjord; mean tide level is ~0.6 m over the open water season, whereas spring tide of up to 1.4 m at outer Clyde Inlet influences the fjordhead to a modest extent (station 3940 Fisheries and Ocean data base, Canada).

## CLIMATE RECONSTRUCTIONS OF NORTHEASTERN BAFFIN ISLAND

Holocene temperature patterns around Baffin Bay show significant regional and temporal variation (Kaplan and Wolfe 2006), making generalizations of the Holocene climate history problematic. Holocene climate of Baffin Island is controlled by declining summer insolation (a decrease of 10% over the last 10 ka; Berger and Loutre 1991), and the decaying LIS (Dyke et al. 2002; Briner et al. 2005, 2007).

A variety of proxy records indicate that the early Holocene was 3 to 4° C warmer than today. Near outer Clyde Inlet, Briner et al. (2006) show a multiproxy lacustrine record in which temperature closely tracked insolation immediately after deglaciation and peaked at ~5° C higher than at present during the early Holocene (10.2–8.5 ka). This warming is also observed in the Agassiz Ice Cap records in the northernmost area of Baffin Bay, which show peak melt between 10.2 and 9.5 ka (Fisher et al. 1995).

Outer Clyde Inlet recorded a distinct cooling of short duration centered at 8.7 ka, which is reflected in only a few other records, e.g., the Agassiz Ice Cap on Ellesmere Island (Fig. 1), as well as marine mollusks in Baffin Bay (Dyke et al. 1996). A marked cold event centered at 8.2 ka is noticeable in several climate proxy records in the Baffin Bay area (Alley et al. 1997). Subsequently, temperatures gradually decline until the last century (Briner et al. 2006).

## DEGLACIATION HISTORY OF NORTHEASTERN BAFFIN ISLAND

The Laurentide Ice Sheet on Baffin Island at the last glacial maximum (LGM) had a jagged margin as shown from evidence of cosmogenic exposure dating of erratic boulders, moraines, and sculpted bedrock (e.g., Miller et al. 2002, Briner et al. 2003, Davis et al. 2006), lake sediments (Miller et al. 2005), and marine data (Gilbert 1985, Dyke et al. 2002). The LIS at its maximum LGM extent consisted of fast-flowing erosive ice streams occupying the main fjords and extending onto the shelf and cold-based, nonerosive ice occupying the high-elevation plateaus as well as the coastal lowlands (Briner et al. 2003, 2005, 2006).

The deglaciation history of Clyde Inlet specifically is well constrained by a combination of cosmogenic and radiocarbon ages (Briner et al. 2007). The LIS retreated from its LGM position on the shelf between 16 and 14 ka (Dyke et al. 2002, Davis et al. 2006). The ice sheet retreated from the nearby coastal lowlands by  $12.5 \pm 0.7$  ka and from the fjord mouth by  $11.7 \pm 2.2$  ka (Briner et al. 2005). Rapid retreat from the outer fjord occurred at  $10.3 \pm 1.3$  ka with the terminus reaching the fjordhead approximately 120 km upstream shortly after 9.4 ka. A widespread readvance after 9.6 ka has deposited distinct moraines (Andrews and Ives 1978). A possible second readvance occurred just before 8 ka (Briner et al. 2007), perhaps corresponding to the 8.2 ka cold event (Alley et al. 1997). A slowly thinning ice lobe persisted in the middle reach of the valley of Clyde River drainage basin until the Middle Holocene, where ages of exposed rock surfaces and perched boulders indicate that ice retreated from ~540 m asl at ~5 ka, from ~400 m asl at 4.7 ka, and from the local valley floor at 320 m asl by 3.5 ka (Briner et al. 2007, 2008). Subsequently, the proto Barnes Ice Cap continued to slowly thin and decay to its present position.

Isostatic rebound has affected all northeastern Baffin Island fjords and caused shoreline displacement and emergence of marine deposits above sea level (Peltier 2004). Clyde Inlet, and nearby Sam Ford Fjord, McBeth Fjord, and Inugsuin Fjord, have emergent marine clays and deltas that delineate an uppermost marine limit up to a topographic elevation of ~70 m asl (Falconer et al. 1965, Løken 1965, Andrews and Ives 1978, Syvitski 1983, Syvitski and Blakeney 1983, Syvitski and Praeg 1984; Fig. 1). Isostatic rebound in Clyde

Fjord was rapid (~0.9–1.1 m/100 yr) during early Holocene, with uplift rates slowing down to 0.15–0.25 m/100 yr over the Late Holocene (Briner et al. 2007). These rates are similar to nearby high-latitude fjords on Baffin Island (e.g., 1.2 m/100 yr for Cambridge Fjord between 8.8 and 6.7 ka; Stravers and Syvitski 1991).

## METHODS

Detailed geomorphological and sedimentological mapping of the glaciofluvial deposits of Clyde River near the fjordhead of Clyde Inlet took place during the summer of 2003. Landsat 7 Enhanced Thematic Mapper Plus imagery and aerial photos of July 1961 at a scale of 1:60,000 are used as a base map. Elevations of geomorphologic units were obtained with Garmin global positioning system (GPS) receivers with an accuracy of  $\pm 3$  m.

Sedimentary pits and sections were described along terrace or riverbank exposures; sediment grain size, color, sedimentary structures, occurrence of shells and organic matter, bed thickness, and nature of contacts between different facies were recorded. We selected five key sedimentary sections that illustrate the sedimentary history of Clyde River valley (Fig. 2), including sections to illustrate the longitudinal and cross-sectional depositional patterns (marked LS and CS, respectively).

Cosmogenic exposure ages from 11 samples and 9 radiocarbon ages provide the chronological framework for the sedimentary system reconstruction (Tables 1 and 2; Briner et al. 2007). Radiocarbon ages (using accelerator mass spectrometry [AMS]) were obtained from marine bivalve and terrestrial organic samples at the Institute of Arctic and Alpine Research (INSTAAR) Laboratory for AMS Radiocarbon Preparation and Research at the University of Colorado, Boulder. The samples are calibrated using CALIB Radiocarbon Calibration html version 5.0.1 (Stuiver et al. 2005). The mean age and one standard deviation were calculated by taking the midpoint of the one standard deviation age range reported in CALIB. Marine samples were calibrated using the CALIB marine database (Hughen et al. 2004) and were corrected for a regional reservoir effect of 540 years obtained from a paired terrestrial organic matter and bivalve sample (Briner et al. 2007). Additional chronological control is provided by four published radiocarbon ages collected from deposits at Clyde fjordhead (Table 2; Andrews and Drapier 1967).

## GEOMORPHOLOGICAL UNITS

### *Ice-Contact Fans (ICF)*

Ice-contact fans from distinct sedimentary landforms along the valley walls of the lower Clyde River valley and are often bordered by kame terraces, and lateral moraines (or trimlines) (Figs. 3A, 4). These features typically span a few hundreds of meters, and their overall shape is somewhat elongated downstream. They are flat-topped with steep side slopes and are covered with large well-rounded boulders (often >1 m) and abundant cobbles and gravel. Elevations of the top surfaces vary between 77 m asl at the coast and 52 m asl 10 km inland. Distributary channels, boulder levees, and midchannel bars are preserved on fan surfaces (Fig. 3B). We interpret the fans as ice-contact features due to their direct contact with side-valley moraine ridges or trimlines, which form distinct along-slope lineaments of unorganized boulders and cobbles. The ice-contact fans were likely deposited at the retreating ice margin while LIS outlet glaciers were still occupying the valley.

### *Marine Mud Deposits (MM)*

Dark-gray muddy deposits occur in large patches over the entire valley floor. They consist of interbedded fine silts and light gray



TABLE 2.—Radiocarbon ages from fjordhead of Clyde Inlet.

Sample number	Sample type	Sample location (as in Fig. 2)	Lat. (N)	Long. (W)	Elevation collected, assoc. marine limit (m asl)	<sup>14</sup> C age ( <sup>14</sup> C yr BP ± 1 SD)	Calibrated and corrected age (cal. yr BP ± 1 SD) <sup>a</sup>
GSC-583 <sup>b</sup>	bivalve	1	69°52'	70°26'	6, 6	2770 ± 140	2770 ± 70
GSC-584 <sup>b</sup>	plant detritus	1	69°52'	70°26'	6, 6	3450 ± 170	3690 ± 210
GSC-631 <sup>b</sup>	bivalve	1–2	69°50'	70°30'	31, ?	6220 ± 140	6910 ± 100
CURL-7043	bivalve	1–2	69°52'	70°24'	20, ?	6680 ± 35	6980 ± 60
CURL-7044	bivalve	2	69°52'	70°26'	43, >49	8120 ± 40	8380 ± 40
CURL-7045	bivalve	2	69°52'	70°26'	48, >49	8700 ± 45	9120 ± 80
I-1932 <sup>b</sup>	bivalve	3	69°52'	70°28'	51, 67	7940 ± 130	8650 ± 190
CURL-7038	bivalve	5	69°50'	70°30'	20, >38	7620 ± 40	7860 ± 40
AA-45381	bivalve	5	69°50'	70°30'	27, >38	7590 ± 70	7860 ± 70
CURL-7039	bivalve	5	69°50'	70°30'	38, >38	7470 ± 40	7730 ± 50
CURL-7046	bivalve	7	69°51'	70°31'	58, >58	8050 ± 35	8330 ± 40
CURL-7040	bivalve	8	69°50'	70°31'	23, 27	6600 ± 35	6880 ± 50
CURL-7041	bivalve	9	69°49'	70°35'	25, 28	7610 ± 35	7880 ± 40

<sup>a</sup> Radiocarbon ages were calibrated using CALIB 5.01, all bivalves were corrected 540 yr for the marine reservoir effect (Briner et al., 2007).

<sup>b</sup> Data from Andrews and Drapier (1967).

### Glaciofluvial Valley Trains and Deltas (GFVT)

Several terraces of unconsolidated sediments occur over the ~2 km width of the Clyde River valley (Fig. 3A). The terrace surfaces tend to cluster within certain elevation ranges (Fig. 4). Directly adjacent to the fjordhead, the highest terrace surface is about 65 m asl; the elevation of lower terraces range between 45 and 20 m asl. Terrace-top surfaces consist of a significant layer of occasional boulders, abundant cobbles, and gravel within a matrix of coarse sand (Fig. 3D). Small remnant channels and braid bars, testifying to high-energy conditions, can be recognized on the top surfaces. The boulder and cobble layers are up to several meters thick. Natural exposures and hand-dug pits show that below the top surfaces sediments consist of homogeneous poorly sorted deposits, in which channel and bar structures are not evidently preserved. At depth, sands grade to finer deposits of laminated fine sands and silts and gradually to marine muds (Fig. 3D). We interpret these units as incised glaciofluvial sandur and delta deposits, which are classified as “valley trains” when they are confined to a narrow bedrock valley like in the Clyde River valley (Benn and Evans 1998). Gradual transitions occur between glaciofluvial sandur deposits and deposits that are classified as glaciofluvial deltas due to the presence of dark marine muds at their base, which have likely been deposited in a prodelta environment.

### Fluvial Terraces (FT)

The elevation of the modern fluvial terrace surfaces range between 11 m asl about 7 km upstream of the river mouth and grade to 0 m asl at the present-day coast (Fig. 4). On this lowermost terrace level, gravels and cobbles form a thin lag deposit at the surface, and sands are situated directly below them (Fig. 3E). Large boulders occur sparsely even on the lowermost terrace levels. Sedimentary sections show a coarsening upward sequence where the deeper deposits are homogeneous fine to very fine sand. Section CS-4 (8 m high) serves as a typical sedimentary sequence of this terrace level. We found no preserved paired shells in the sands, although eroded shell fragments do occur. A number of sandy midchannel bars and mouth bars are part of the active depositional system of Clyde River today. Close to the present-day river mouth, remnants of older sandy beach ridges and

strand lines are recognized up to 6 m asl. This elevation is too high to reflect present-day tidal variation and is interpreted as the result of ongoing, slow, isostatic uplift.

These lowermost terraces are interpreted to be fluvial terraces of the modern Clyde River. Generally finer grain sizes of deposited sands point to decreased fluvial transport capacity during deposition. The sparse boulders and cobbles are interpreted as originating from the local valley slopes or as being reworked from higher glaciofluvial terrace levels during incision.

### SEDIMENTARY SEQUENCES

Three sedimentary logs at the fjordhead of Clyde Inlet (locations 2, 3, 4; Fig. 2) illustrate the cross-sectional sedimentary sequence of the valley fill (Fig. 5A). The highest sedimentary section (CS-3) has its top at 64 m, whereas this terrace level overall is measured at ~67 m asl. There are meter-scale variations in the elevation measurements and the estimation of the overall surface level, both due to GPS accuracy (±3 m) and due to local bar and channel morphology on the ICF surfaces. CS-2 has its top at 48 m asl; CS-4 starts at 8 m asl (Fig. 5A).

At the highest level (CS-3) a >1-m-thick layer of cobbles and gravel comprises the terrace surface, below which are about 7 m of very coarse to coarse sands with abundant small pebbles. Two distinct ~40-cm-thick horizons of clay interlayered with silts occur at ~62 m asl and ~59 m asl. The millimeter-scale layering in these deposits points to a temporarily quiet depositional environment.

A few hundred meters downslope, section CS-2 provides exposure of the lower units of the same sequence. Here, most deposits are significantly finer grained. The uppermost 2 m of the sedimentary section consists of crumbly dark clays directly overlain by terrace gravels. Some soil formation and rooting has taken place throughout both the clay and terrace gravel deposits. This layer is interpreted to be reworked sediments originating locally from somewhat higher up the slope, which is corroborated by an anomalous date on a bivalve sample of 9120 ± 80 calibrated (cal) years before present (BP). We speculate that the fine-grained layers at ~62 m or ~59 m asl identified in section CS-3 potentially formed the source for these reworked sediments. Two small coarsening upward sequences occur, with small slump structures indicative of sediment deformation. Overall, this part

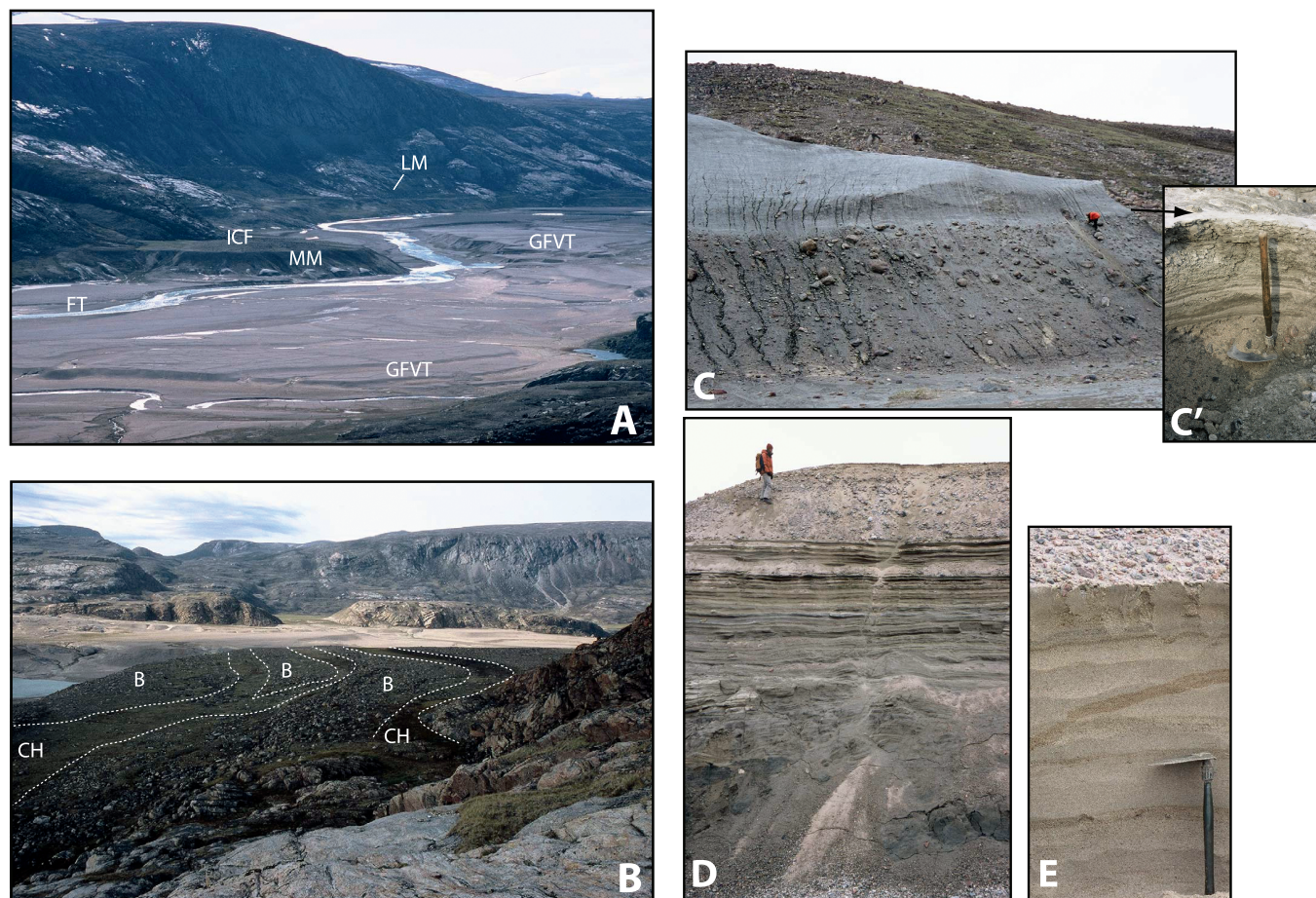


FIG. 3.—**A**) View upvalley  $\sim 3.5$  km landward of the present-day river mouth. The major geomorphological units can be distinguished: Ice-contact fan (ICF), Lateral moraines and kame terraces (LM), Glaciofluvial valley train complexes (GFVT), Glacio-marine deposits (MM), and the lowermost fluvial terrace (FT). **B**) Looking upon the ice-contact fan visible in Figure 3A. A relatively flat-top surface shows preserved boulder-strewn bars (B) and shallow channels (CH). Samples for cosmogenic dating were taken from this surface (Table 1). **C**) Example of a lobe of glacio-marine muds (MM) draped directly upon the ice-contact fan. The abrupt contact of the marine muds on coarser sediments and pebbles is shown in the inset figure C', shovel length is 0.5 m. The photo (C') is taken at another exposure at the side of this deposit,  $\sim 25$  m laterally from the pit in 3C. **D**) Terrace sidewall exposure of glaciofluvial valley train deposits showing dark clays at the base, alternated layers of silts and sands, and coarse topset deposits. Person 1.75 m for scale. **E**) Excavated section in lowermost fluvial terrace. Shovel is  $\sim 0.5$  m length. Note the thin pebble lag at the surface, and absence of coarse material in the fine sands directly below the surface.

of the sequence shows few-millimeter to 1-cm-scale horizontal layers. At the base a  $>1.5$ -m-thick interbedded clay and silt layer of marine bivalves has a radiocarbon age of  $8380 \pm 40$  cal years BP. Glaciofluvial and marine sediments form several lower terrace levels. Briner et al. (2007) dated marine bivalves from exposed marine muds at 20 and 31 m asl to  $6910 \pm 100$  and  $6980 \pm 60$  cal years BP, respectively. Marine shells sampled at incised marine mud deposits at 6 m asl are  $3690 \pm 210$  and  $2770 \pm 140$  cal years BP (Andrews and Drapier 1967; Table 2). Because there are a number of nondistinct terrace levels it is difficult to tie each of these samples to their precise contemporaneous sea level. In addition, bivalves of the *Portlandia* association typically occur over a large depth range in shallow marine (5–40 m) arctic environments (Aitken and Fournier, 1993), which induces further uncertainty in obtaining a precise sea-level estimate from the samples.

Section CS-4 forms a typical sedimentary log of the lowermost fluvial terrace level (Fig. 5A). The top 20 cm of CS-4 consists of reworked marine muds that have been rain-washed onto the present-day surface and were disregarded in the interpretation of the depositional history. Below the muds are 2.5 m consisting of a few cobble- and gravel-rich layers interbedded with poorly sorted sediments. The lowermost 4 to 5 m of this section consists of a meters thick layer of homogeneous very fine sands.

Two additional sedimentary logs at 7 km (LS-9) and 3 km (LS-8) upstream from the river mouth illustrate the longitudinal pattern in the sedimentary sequence (Figs. 5B, 6, 7).

Both these sections can be related to a nearby ICF complex or tied to a persistent surface elevation marked by lateral moraines. Furthest upstream, LS-9 in Figures 5B and 6, about 7 km from the present-day river mouth, ICF complex deposits are not volumetrically significant, although narrow kame terraces or lateral moraines (LM) form a

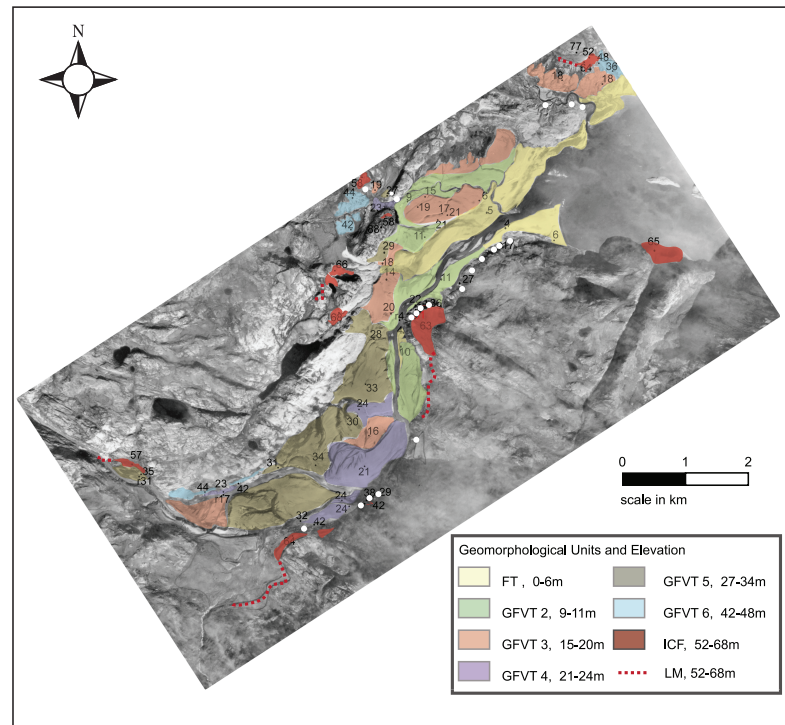


Fig. 4.—Map of the geomorphological units at Clyde fjordhead, Baffin Island, Canada. Ice-contact fans (ICFs) and associated lateral moraines (LM) and kame terraces are shown. Exposed marine muds (MM) draped directly onto ICFs are indicated with small circles. The incised glaciofluvial valley trains and deltas (GFVTs) have been mapped by identifiable surfaces in distinct elevation ranges. GFVT units grade into marine muds at their base. Lowermost terrace level and the active modern river bed (FT) is distinct at 0–6 m.

lineament on the opposite, north side of the valley (marked on Fig. 3A). The highest exposed marine muds draped onto bedrock here are at 42 m asl. Sedimentary section LS-9 (Figs. 5B, 6) is part of sedimentary deposits extending steeply downward from 37 m asl to the present river level. Between the top of the exposure at 28 and 25 m asl, dark clays are interrupted by a few-decimeter-scale silt layers. The silt layers have an abrupt contrast with the underlying muds, but it is unclear whether they were erosive. Silt layers are thicker and more frequent in the top of the section. We interpret the silt layers as turbidity current deposits, common in fjord environments (e.g., Prior et al. 1987, Storms et al. 2012), because these sediment beds are coarser-grained than the matrix sediments, display grading, and display both parallel laminations as well as deformed ripples and flames.

Marine bivalves retrieved from the clays in the lower part of this interval are  $7880 \pm 40$  cal years BP (Fig. 6; Table 2). Small pebbles occur frequently in the clays, and are interpreted as dropstones. A 1.5-m-thick coarsening upward sequence at  $\sim 24$  m grades from dark clays to clays interbedded with centimeter-scale sand to fine sand layers. At the base of the exposure  $\sim 2$ -m-thick beds of fine to medium sand with a number of deformed large clay lenses grade into clays and interbedded silts. In addition, ripples or small flame structures in the fine sands point to deposition by gravity flows. There is also evidence for deformation, loading, and shearing in these fine sands, perhaps just part of the mass flow process or testament of ice overriding these sediments.

Log LS-8 is located more downstream, near the location of photo 3D on the northern side of Clyde River just opposite the ICF complex at location 6. The sedimentary log is depicted in Figure 5B, photos of

selected characteristic intervals are shown in Figure 7. The top surface of the associated ICF complex (62 m asl) has been cosmogenically dated at  $\sim 7.6$  ka. Marine clays draped directly onto the ice-contact fan slopes were sampled for bivalves at 38, 27, and 20 m asl (location 5 in Fig. 2). The bivalve samples date to  $7890 \pm 40$ ,  $7860 \pm 70$ , and  $7730 \pm 50$  cal years BP, respectively.

The relative position of the terraces near LS-8 indicates that these are the subsequent depositional landforms of this sedimentary sequence. LS-8 forms one of the longest sections described and is used to illustrate sedimentary patterns of the infill; it shows a gradual coarsening upward sequence with several meters of crumbly dark clays comprising decomposed seaweeds at its base grading to laminated clays (Fig. 7D). Marine shells date the basal clays at an elevation of 13 m asl at  $6880 \pm 50$  cal years BP. A 6-m-thick package of horizontal interbedded silts and very fine sands alternates with sets of more homogeneous sands. The layering varies from millimeter-scale laminae in silt-rich intervals (Fig. 7C) to centimeter-scale laminae in fine sandy intervals (Fig. 7B). This rhythmic bedding could be attributed to tidal influence, but we observed no neap-spring successions. Rather, we attribute the rhythmic bedding to seasonal variation in river discharge that drives suspension plumes, similar to varve deposits in high-latitude lakes (Benn and Evans 1998). Thin clay-silt couplets are the most distal expression of the seasonal suspension fall-out deposits, and the silt-sand couplets are deposited more proximal to the river mouth. The layered package is overlain by a thick layer of poorly sorted coarse sand with abundant gravel and cobbles, especially near the terrace surface at 27 m asl (Fig. 7A). Figure 8 summarizes the stacking of the different units and the local

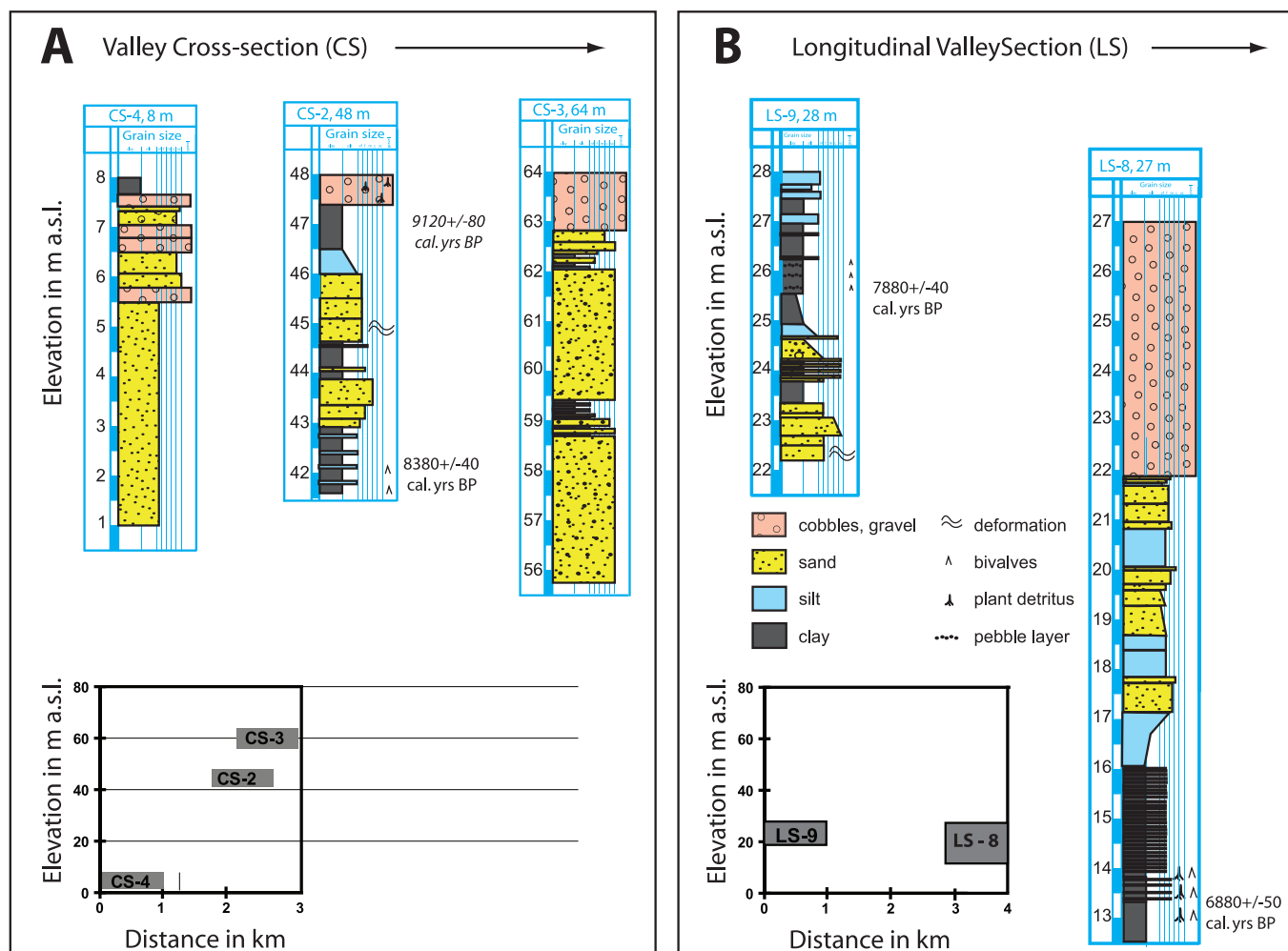


FIG. 5.—A) Sedimentary logs through locations 3, 2, 1, and 4, forming a typical cross-valley section (CS, as indicated in Fig. 2). B) Sedimentary logs at locations 8 and 9, illustrating sedimentary patterns in longitudinal direction (LS as indicated in Fig. 2).

small variations in their superposition from upstream to downstream direction.

## INTERPRETATION OF SEDIMENTARY EVOLUTION

### *Sequence Stratigraphic Model for Fjord Valleys*

Conceptual models for fjord valley fills by Corner (2006) and Schack Pedersen (2012) are helpful in describing the sedimentary evolution of the Clyde Inlet fjordhead. It contains a “deglacial stage,” when the sedimentary system is still influenced by an active ice sheet. The deglacial stage is further subdivided into two phases (1) “a fjord–glacier stage” where a marine-terminating or tidewater glacier regime exists, and (2) “a valley glacier stage” during which time the ice sheet has become grounded, or land-terminating, and sands and gravels are delivered to the head of the fjord by glacier-fed rivers. The “postglacial stage” of valley filling starts after the waning ice sheet retreats from the headwaters of the river drainage basin. During this phase the sediment supply can be drastically lowered, and the rain- and snow-fed river becomes the sole medium of sediment transport.

### *Deglacial Stage at Clyde Fjordhead*

The ice stream in Clyde Inlet rapidly retreated from the outer fjord from  $10.3 \pm 1.3$  ka and reached the fjordhead approximately 120 km upstream shortly after 9.4 ka (Briner et al. 2007). The present depth of Clyde Inlet suggests that rapid ice retreat was due to calving dynamics and would have occurred during peak temperatures of the Holocene thermal maximum identified in local climate proxies at 10.2–8.5 ka (Briner et al. 2006). Once the outlet glacier became grounded in the Clyde River valley, retreat rates decreased. The middle reaches of the Clyde River drainage basin, 30 km upstream of the fjord head, became ice free  $\sim 3.5$  ka (maps in Briner et al. 2007).

The valley fill at Clyde fjordhead is bounded below by bedrock, revealed by locally exposed bedrock at topographic highs. There are no seismic data available for this fjord system, but the bedrock depth in the longitudinal direction is likely variable with overdeepened pockets at paleo ice stream confluences (McGregor et al. 2000). Thus, bedrock troughs form the lower sequence boundary but induce significant variation in infill thickness along a longitudinal fjord profile. We found no significant exposures of older overridden sediments, i.e., diamicton, although it is hypothesized to possibly

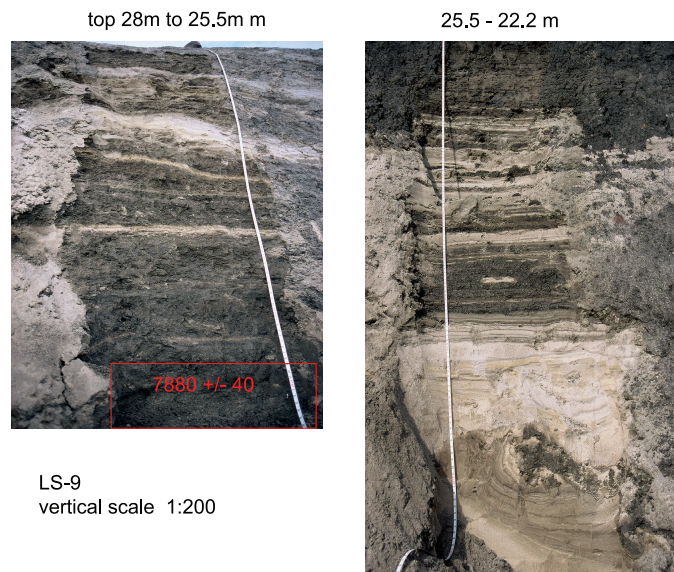


FIG. 6.—Sedimentary structures of log LS-9, showing marine muds interbedded with silt layers displaying parallel lamination and flame structures. Sample CURL-7041 consisted of bivalves originating from the dark bioturbated muds, and dated to 7880 cal yr BP. At the base of this sedimentary section a thicker layer of very fine to fine sands occurs with pronounced deformation likely indicative of a gravity flow, perhaps associated with a small ice advance.

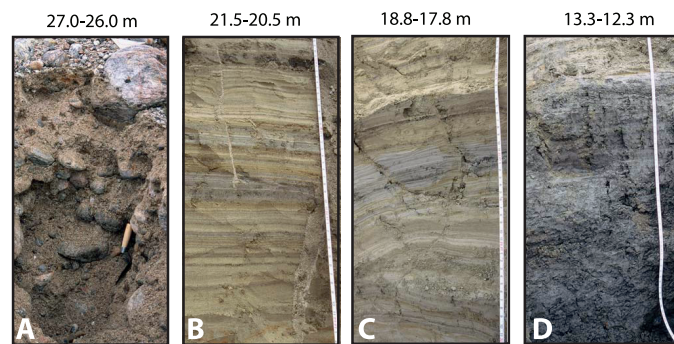


FIG. 7.—Sedimentary structures within the GFVT units of sedimentary log LS-8, all photos cover a 1-m interval. This section is taken at the location depicted in Fig. 3D. **A)** Coarse poorly sorted sands with abundant cobbles and some small boulders. **B)** Rhythmic lamination of centimeter-scale coarse to fine sand couplets, probably caused by seasonal discharge variation. **C)** Rhythmic lamination of centimeter- to millimeter-scale fine sand and silt couplets, probably caused by seasonal discharge variation. A few lenses of coarser sand occur, associated with higher energy turbidity events. **D)** Silt-clay laminated sediments grading downward to massive, bioturbated dark clays with occasional shells and decayed organic matter.

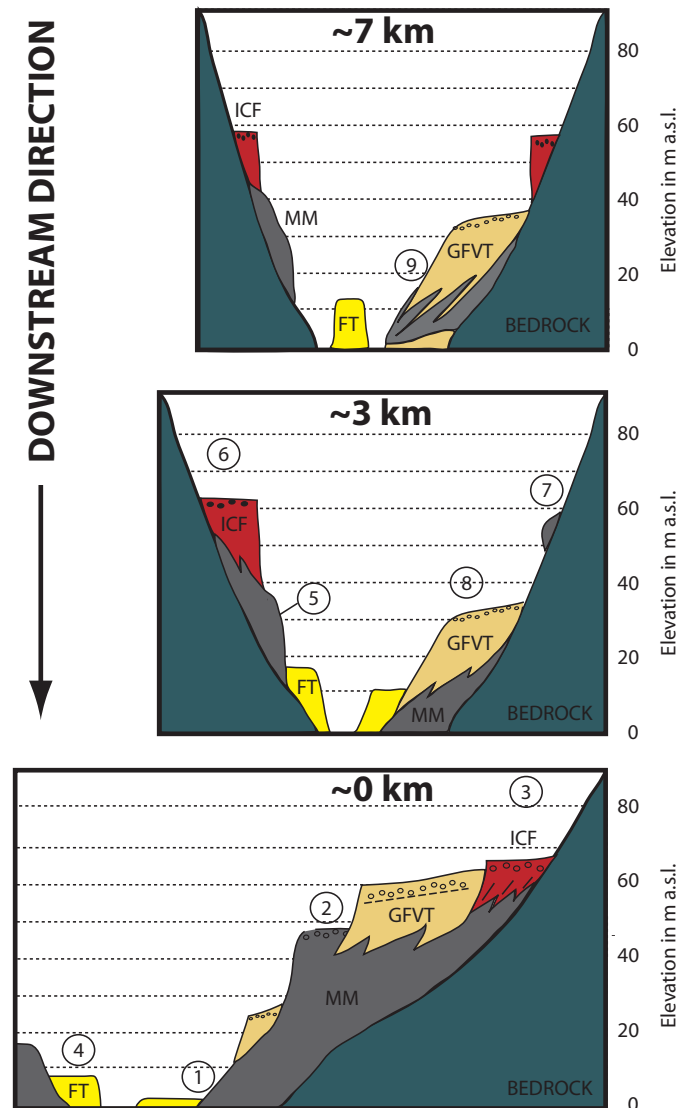


FIG. 8.—Schematic valley cross-sections at  $\sim 7$  km,  $\sim 3$  km, and near the river mouth. The numbers refer to the sedimentary logs (Fig. 5) and sample locations listed in Tables 1 and 2.

occur in the subsurface at sheltered locations. Marine seismic data of nearby fjords on northeast Baffin Island show minor volumes of till and other preserved sediments of pre-LGM valley fill deposits near sills and irregularities in the bedrock valley floor that escaped erosion of the latest LGM ice streams (Gilbert 1985).

We have developed a sequence stratigraphic model for the sedimentary evolution of Clyde fjordhead (Fig. 9). Ice-contact fans were being deposited at early stages of the valley fill, (Fig. 9), the highest surface of which lies  $\sim 67$  m asl, close to the fjordhead; similar ice-contact fan surfaces lie at 64, 65, 62, and 57 m asl further upstream (Figs. 2, 4). These surfaces are assumed to represent relative sea level at the time of their deposition (the elevation of the preserved fan surface is assumed to grade to within  $\sim 2$  m above mean base level at the time, which is referred to as the marine limit). As stated above, the highest surface elevation at which a graded ICF surface is recognized in the Clyde fjordhead region lies at 67 m asl, which

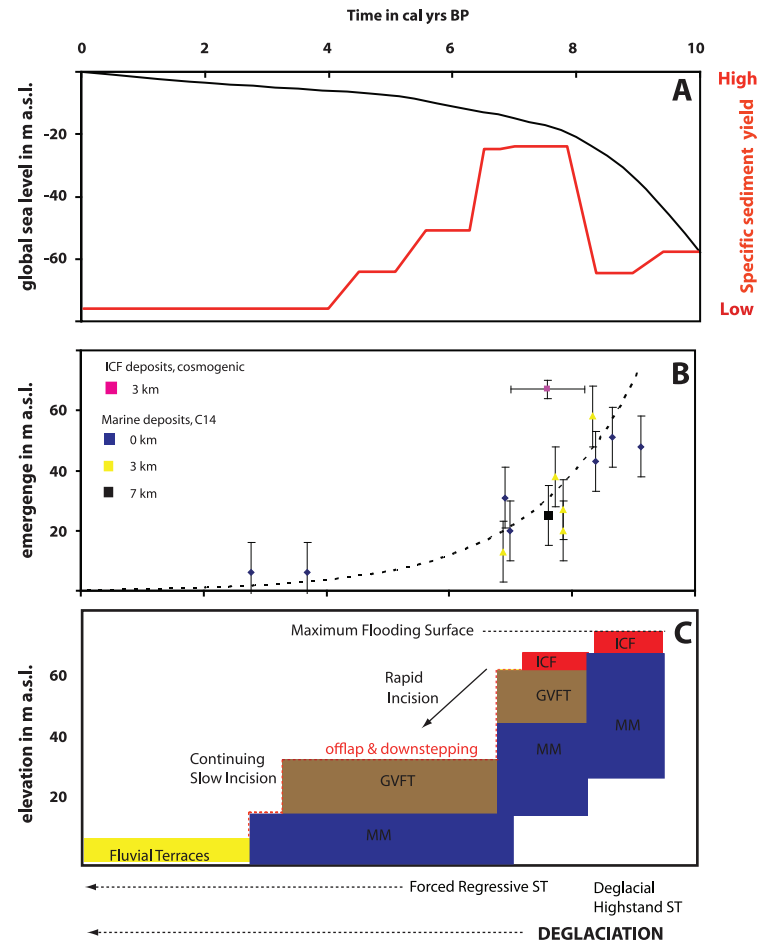


FIG. 9.—Conceptual model of controlling factors and the valley fill in Clyde fjordhead. **A)** Global sea-level curve (modified after Lambeck and Chappell 2001) indicating sea-level rise (solid black line). Sediment supply curves based on geographic information system reconstruction of terrace volumes (solid red line) support the paraglacial sediment cycle concept (after Church and Ryder 1972). Sediment yield peaks shortly after deglaciation and drops relatively rapidly afterward or remains high for an extended period afterward when the fluvial system still carries down previously stored paraglacial sediment. **B)** Emergence curve for Clyde fjordhead based on elevation of the collected samples. Marine deposits have  $\pm 10$  m whiskers attached that illustrate their relative uncertain position as associated to contemporaneous sea level. ICF surfaces are assumed to grade to contemporaneous sea level and have only  $\pm 3$  m measurement uncertainty. The regression of all data combined shows an exponential emergence curve,  $y = 0.34e^{0.0006x}$  and associated  $R^2$  of 0.85. **C)** Depositional units and sequence stratigraphic boundaries as related to the controlling factors over time.

corresponds to the maximum extent of fjord inundation and is as such the maximum flooding surface in a sequence stratigraphic sense (Fig. 9).

Rapid inundation of the fjordhead due to global sea-level rise (Fig. 9A) coincides with the initial depositional phase, which is corroborated by abrupt contacts between ice-contact fans and deposits of marine muds. Basal glacio-marine muds are found directly above the bounding bedrock, but they also drape abruptly on the ICFs. Andrews and Drapier (1967) dated bivalves from marine muds associated with a 67 m asl marine limit near the river mouth to 8.6 ka. We speculate that a layer of reworked muds with an age of 9.1 ka also relates to the marine limit at  $\sim 67$  m asl. In addition, isolated mud draped onto bedrock at 58 m asl is dated at 8.3 ka. These glacio-marine mud deposits drape directly onto either the ICFs or bedrock and can be attributed to the deglacial highstand system tract (DHST in Fig. 9).

Glaciofluvial valley trains were then deposited when the ice margin continued retreating (Figs. 8, 9). Surface dips of the early GVFT surfaces indicate that forced regression began almost immediately after the highstand. The highest surface elevation of the glaciofluvial valley trains close to the fjordhead is at 62 m asl. This terrace surface grades steeply to 48 m, testifying to rapid uplift and possibly some lag time before sediment supply peaks. The associated prodelta marine muds are dated with marine bivalves to 8.4 ka.

Another ICF complex at 3 km inland from the fjordhead testifies to a stagnating ice margin or perhaps of a readvance of the ice margin. The top surface of the ICF at 65 m was dated with cosmogenic exposure techniques to  $\sim 7.6$  ka, and bivalves from the marine muds that are directly draped upon the ICF slopes are dated to 7.9 cal ka BP. Thus, the ICF was most likely deposited just prior to 7.9 ka. In addition, deformed turbidite sands at the base of the sedimentary section at  $\sim 7$  km upstream may have possibly been overridden by

readvancing ice, which perhaps deposited this ICF complex. This unit must have been formed well before 7.9 ka as evidenced from dated bivalves. Both sedimentary features may have been deposited around the 8.2 ka cold event (Alley et al. 1997), which appeared to have impacted Baffin Island (Miller et al. 2005). Briner et al. (2006) reconstructed an additional cold period  $\sim 8.7$  ka from lake sediments near the hamlet of Clyde River near the outer fjord (indicated with a star Fig. 1). Either cold period could have resulted in a readvance of the local ice tongue of the LIS near Clyde fjordhead. These short-lived cold periods have a profound influence on the valley fill stratigraphy, as the associated coarse-grained ICFs amalgamate directly with the prograding packages of coarse sandy glaciofluvial valley trains.

Successive glaciofluvial terrace levels and associated prodelta muds grade down to lower relative base-level elevations with falling sea level due to isostatic rebound. We assume that sandur surfaces spanned the valley floor. Despite subsequent incision, these sediments comprise relatively large volumes of the valley fill. They all form part of the sediment pulse that is transported within a few thousand years after deglaciation (Fig. 9A). These deposits all form an accretionary forced-regressive system tract (FRST; sensu Helland-Hansen and Gjelberg 1994, Corner 2006). The age of the early GFVTs and associated delta sediments coincides with the Holocene thermal maximum, when high melt rates of the ice sheet in the hinterland would have led to high river discharge. We speculate that the retreating tongues of the proto Barnes Ice Cap still had a warm-based erosive regime. Subsequent incision of the Clyde River removed parts of the sandy valley fill. Relative sea level is documented by elevations of dated prodelta muds and sea level drops from 31 and 20 m asl (at 6.9 ka and 7.0 ka) to 6 m asl (at 3.7 and 2.8 ka) (Fig. 9B). The water depth range of living bivalves is considerable, making it uncertain to tie their elevation to a precise marine limit; however, an exponential shape of the emergence curve fits the data ( $E = 0.34e^{0.0006t}$ ,  $r^2 = 0.85$ ).

#### *Postglacial Stage at Clyde Fjordhead?*

The lowermost suite of terraces between 11 and 0 m asl are interpreted as recent fluvial terraces based on the absence of boulders and thick layers of cobbles. They mostly consist of well-sorted medium sands. Close to the present coast there are a few minor beach ridges. The volume of the fluvial terrace deposits is much lower than the GFVT deposits.

Similar recent fluvial terraces have been described in valley fills in East Greenland (Hansen 2004) and Norway (Helle 2004, Corner 2006, Eilertsen et al. 2007), which are deposited after the ice sheet retreated from the watershed boundaries and classified as the “postglacial system tract.” However, the Clyde fjordhead has not entered a “postglacial stage sensu stricto,” which is defined by the decoupling of the glacial ice from the drainage basin, because the Barnes Ice Cap meltwater still drains into the drainage basin. It is evident from the  $^{10}\text{Be}$  dated bedrock in the middle reaches of the Clyde drainage basin that a thinning ice lobe persisted until well into the Middle Holocene in a large part of the drainage basin.

Apparently, sediment supply toward Clyde fjordhead was greatly reduced despite a continuous hydrological connection to a hinterland ice cap. There is no doubt that a string of upstream lakes along the 66 km river stretch plays a role in sediment trapping. However, we suspect that the retreating proto Barnes Ice Cap switched its mass-balance regime over this period; it most probably changed from a more erosive, warm-based ice lobe to a cold-based thinning ice cap. A more warm-based glacier regime would produce a much higher sediment pulse to the Clyde River. In addition, we attribute low sediment supply rates to the polar desert climate of the site, which reduces the Barnes Ice Cap meltwater flux as well as annual snow and rain in the drainage area and as such limits the water transport capacity of the Clyde River system.

## DISCUSSION

Late Quaternary valley deposits illustrate a rapid infill after the melting Laurentide Ice Sheet withdraws from the fjordhead of Clyde Inlet. We find a coarsening upward stratigraphic pattern to be unique for valley fills in high latitudes as compared with typical fining upward sequence in incised valleys in lower-latitude environments. Even at the lowest latitude margins of the Pleistocene Ice sheets, for example in Denmark and northern Germany, a dominantly coarsening upward sequence results from deglacial deposition (Schack Pedersen 2012).

The glacially scoured bedrock valley forms the sediment sink and defines the lower sequence boundary. During the “deglacial stage,” the valley fill was controlled by ice retreating within the Clyde River basin. Moraines and bouldery, coarse-grained ice-contact fans are interpreted as being deposited at the retreating ice sheet margin. ICF surfaces are covered with small boulder levees and channels that presumably grade to contemporaneous base level. The top surfaces of these fans define the highest elevation and oldest deposits of the valley fill deposits. Along the longitudinal valley profile of the Clyde fjordhead a number of isolated coarse-grained ICF complexes were deposited at the ice margin during short stagnations in its retreat. The oldest and highest ICF complex at the fjordhead dates 9.2 ka, and a well-developed, somewhat lower ICF  $\sim 3$  km upstream is  $\sim 8$  ka. The younger ICF may be associated with renewed ice-contact sedimentation after a readvance of the ice sheet due to the short-lived 8.2 ka cold event. Thus, fjord valley infills can be uniquely distinguished from classic valley fill sequences that gradually fine upward by the significant volumes of very coarse-grained deposits that occur at relatively high elevations in the valley fill sequence. In the Clyde fjordhead, ICF complexes form the highest elevation surfaces.

In many occurrences, we found glacio-marine mud deposits draped directly onto the ICF complexes or onto bedrock, which corresponds to the maximum extent of marine inundation, and are as such the classical maximum flooding surface in a sequence stratigraphic sense.

High along the valley slopes, sandy glaciofluvial deltas and valley trains were being deposited when the ice margin continued retreating and local river systems became active. Thick layers of sand and coarse sand grade into cobble- and boulder-covered GFVT surfaces. These glaciofluvial sediments contribute additional large volumes of coarse sandy sediments within the downstepping valley fill sequence. Lower down within the same GFVT units, distinct rhythmic clay-silt and fine sand-silt couplets resulting from seasonally varying suspension flows occur. Rare occurrences of small-scale turbidite deposits have been found, but in the exposures of this study gently dipping foreset slopes prohibit extensive occurrence of turbidity currents. Dark, bioturbated marine muds with shells and occasional organic matter occur at the base of the GFVT units. The GFVT deposits in their entirety form a large part (volumetrically) of the valley fill and consist of the FRST. Stravers et al. (1991) reconstruct a mass balance of valley fills in sandurs elsewhere on Baffin Island, showing that a fill consists of 10% till or diamicton, 50% glaciofluvial and deltaic sediments, and 40% glacio-marine deposits. The Clyde terraces decrease in elevation over time under conditions of sea-level fall, which was as rapid as 20 m/ka between 9 and 7 ka. Dip angles of the older GFVT surfaces indicate that forced regression due to sea-level fall began almost simultaneously with the onset of deposition. For example, the highest surface level of the glaciofluvial valley trains close to the fjordhead starts at 62 m asl inset into the slopes of the highest ICF. This terrace surface dips rather steeply to 48 m. Farther upstream, the GFVT surface grades to  $\sim 28$  m at the lowest associated marine muds, which grade to 6 m asl. Downstepping indicates that sea-level fall remains dominant over sediment supply even in this phase of major sediment transport with high meltwater rates from the hinterland (Fig. 9), and thus the FRST remains accretionary.

The importance of ongoing sea-level fall and the fact that sediment supply cannot keep up is even more striking when the river started incising its fill (Fig. 9). Large volumes of previously deposited GFVTs have been eroded. Clyde River at present is still influenced by the Barnes Ice Cap, a remnant of the Laurentide Ice Sheet, so we conclude that it may not be necessary to enter a postglacial phase *sensu stricto* to initiate a phase of major incision. Apparently, rapid uplift after deglaciation causes a river system to significantly incise despite continuing sediment supply. A waning hinterland ice cap may not produce sufficient sediment as compared with more active mountain glaciers, which the Clyde River basin lacks. Moreover, proglacial lakes at the front of the waning ice lobe effectively capture most of the bedload. Syvitski et al. (1987) point out the importance of sediment trapping of larger Arctic drainage basins, where discharge is modulated by lakes, resulting in better sorting and decreased bedload transport. The lakes disconnect sediment sourced by the Barnes Ice Cap retreat from the fluvial system. Remaining suspended load is likely to be transported but can have easily been bypassing the incised fluvial valley.

During the last phase of the valley fill, isostatic rebound and consequently sea-level fall slows down by an order of magnitude. Still, the Clyde River system is incising into its own deposits. Narrow ribbons of sandy fluvial terraces were being deposited along the river channel, stratigraphically close to the lower sequence boundary.

We conclude that stratigraphic patterns of valley fills are unique in high-latitude areas. The erosional lower bounding surface is likely well constrained, whether this be carved bedrock or the lowermost excavation surface (Kalefa El-ghali 2005, Janszen et al. 2013). Old, coarse ICF sediments occur relatively high along the valley slopes; marine silts and muds interfinger at all levels of the fill sequence; and ribbons of young sandy fluvial sediments occur stratigraphically low near the original lower sequence boundary due to incision. The resulting stratigraphy is patchy and complex, depending on the exact interplay of the rates of local sea-level change and sediment supply. However, in ancient glaciogenic systems, conglomeratic layers, presumably originating from ICFs, are expected to be associated with downstepping sandy GFVTs. These sandy deposits may comprise significant volumes, since they originate from the most active sediment producing phase of deglaciation. It is clear from this study that glacial valley fill systems recognized in ancient outcrop studies need to be disentangled carefully. The interplay of sea-level change, isostatic rebound, and climate's influence on sediment supply in individual fjord valleys may result in distinctly different sedimentary infills.

## ACKNOWLEDGMENTS

We thank T. Davis and J. Leonard who assisted in the field and J. Turnbull for preparation of radiocarbon samples. We thank the Nunavut Research Institute and the people of Clyde River, particularly J. Qillaq and J. Hainnu, for assistance with field logistics. We thank J. Andrews, G. Miller, and A. Jennings for stimulating discussions on the sedimentary history of Baffin Island. J. Jacobs kindly shared climatological data and insights on the Barnes Ice Cap.

We thank our reviewers: W. Helland-Hansen provided valuable comments on this manuscript and G. Corner and J. Menzies helped with an early version of this manuscript. This research project was funded by the US National Science Foundation, NSF-OPP, Arctic Natural Sciences program.

## REFERENCES

- Aitken AJ, Fournier J. 1993. Macrobenthos communities of Cambridge, McBeth and Itirbilung fjords, Baffin Island, Northwest Territories, Canada. *Arctic* 46(1):60–71.
- Alley RB, Mayewski PA, Sowers T, Stuiver M, Taylor KC, Clark PU. 1997. Holocene climatic instability: A prominent, widespread event 8200 yr ago. *Geology* 25:483–486.
- Andrews JT. 1987. Late Quaternary marine sediment accumulation in fiord-shelf-deep-sea transects, Baffin Island to Baffin Bay. *Quaternary Science Reviews* 6(3–4):231–243.
- Andrews JT, Drapier L. 1967. Radiocarbon dates obtained through Geographical Branch field observations. *Geographical Bulletin* 9:115–162.
- Andrews JT, Ives JD. 1978. “Cockburn” nomenclature and the late Quaternary history of the eastern Canadian Arctic. *Arctic and Alpine Research* 20:617–633.
- Ballantyne CK. 2002. Paraglacial geomorphology. *Quaternary Science Reviews* 21:1935–2017.
- Benn DI, Evans DJA. 1998. *Glaciers and Glaciation*: Hodder Arnold, London. 744 p.
- Berger A, Loutre MF. 1991. Insolation values for the climate of the last 10 million years. *Quaternary Science Reviews* 10:291–310.
- Briner JP, Michelutti N, Francio DR, Miller GH, Axford Y, Wooler MJ, Wolfe AP. 2006. A multi-proxy lacustrine record of Holocene climate change on northeastern Baffin Island, Arctic Canada. *Quaternary Research* 65:431–442.
- Briner JP, Miller GH, Davis PT, Bierman PR, Caffee M. 2003. Last Glacial Maximum ice sheet dynamics in Arctic Canada inferred from young erratics perched on ancient tors. *Quaternary Science Reviews* 22:437–444.
- Briner JP, Miller GH, Davis PT, Finkel R. 2005. Cosmogenic exposure dating in arctic glacial landscapes: Implications for the glacial history of northeastern Baffin Island, Arctic Canada. *Canadian Journal of Earth Sciences* 42:67–84.
- Briner JP, Miller GH, Finkel RF, Hess DP. 2008. Glacial erosion at the fjord onset zone and implications for the organization of ice flow. *Geomorphology* 97(1–2):126–134.
- Briner JP, Overeem I, Miller G, Finkel R. 2007. The deglaciation of Clyde Inlet, northeastern Baffin Island, Arctic Canada. *Journal of Quaternary Science* 22(3):223–232.
- Centre for Topographic Information. 1998. Canadian Digital Elevation Data, Level 1 (CDED1). <http://www.GeoBase.ca>. Accessed March 3, 2017.
- Church M. 1972. *Baffin Island Sandurs: A Study of Arctic Fluvial Processes*, Bulletin 216: Geological Survey of Canada, Ottawa, Ontario. 208 p.
- Church M, Ryder JM. 1972. Paraglacial sedimentation: A consideration of fluvial processes conditioned by glaciation. *Geological Society of America Bulletin* 83:3059–3071.
- Church M, Slaymaker O. 1989. Disequilibrium of Holocene sediment yield in glaciated British Columbia. *Nature* 337:452–454.
- Corner G. 2006. A transgressive–regressive model of fjord-valley fill: Stratigraphy, facies and depositional controls. In Dalrymple RW, Dale AE, Tillman RW (Editors). *Incised Valleys in Time and Space*, Special Publication 85: SEPM (Society for Sedimentary Geology), Tulsa, Oklahoma. p. 161–178.
- Dalrymple RW, Boyd R, Zaitlin BA (Editors). 1994. *Incised-Valley Systems: Origin and Sedimentary Sequences*, Special Publication 51: SEPM (Society for Sedimentary Geology), Tulsa, Oklahoma. 391 p.
- Dalrymple RW, Dale AE, Tillman RW (Editors). 2007. *Incised Valleys in Time and Space*, Special Publication 85: SEPM (Society for Sedimentary Geology), Tulsa, Oklahoma. 348 p.
- Davis PT, Briner JP, Coulthard RD, Finkel RC, Miller GH. 2006. Preservation of arctic landscapes overridden by cold-based ice sheets. *Quaternary Research* 65(1):156–163.
- de la Grandville BF. 1982. Appraisal and development of a structural and stratigraphic trap oilfield with reservoirs in glacial and periglacial clastics. In Halbouty MT (Editor). *The Deliberate Search for the Subtle Trap*, Memoir 32: American Association of Petroleum Geologists, Tulsa, Oklahoma. p. 267–286.
- De Winter I, Storms JEA, Overeem I. 2012. Numerical modeling of glacial sediment production and transport during deglaciation. *Geomorphology* 167–168:102–114.
- Dyke AS, Andrews JT, Clark PU, England JH, Miller GH, Shaw J, Veillette JJ. 2002. The Laurentide and Innuitian ice sheets during the Last Glacial Maximum. *Quaternary Science Reviews* 21:9–31.

- Dyke AS, Dale JE, McNeely RN. 1996. Marine mollusks as indicators of environmental change in glaciated North America and Greenland during the last 18,000 years. *Géographie Physique et Quaternaire* 50:125–184.
- Eilertsen R, Corner GD, Aasheim O, Andreassen K, Kristoffersen Y, Ystborg H. 2007. Valley-fill stratigraphy and evolution of the Målselv fjord valley, northern Norway. In Dalrymple RW, Dale AE, Tillman RW (Editors). *Incised Valleys in Time and Space*, Special Publication 85: SEPM (Society for Sedimentary Geology), Tulsa, Oklahoma. p. 179–195.
- Falconer G, Andrews JT, Ives JD. 1965. Late-Wisconsin end moraines in northern Canada. *Science* 147:608–610.
- Fisher DA, Koerner RM, Reeh N. 1995. Holocene climatic records from Agassiz Ice Cap, Ellesmere Island, NWT, Canada. *The Holocene* 5:19–24.
- Gilbert R. 1985. Quaternary glaciomarine sedimentation interpreted from seismic surveys of fjords on Baffin Island, N.W.T. *Arctic* 38(4):271–280.
- Guymon GL. 1974. Regional sediment analysis of Alaskan Streams. *Journal of Hydraulics Division, Proceedings of the American Society of Civil Engineers* 100:41–51.
- Hallet B, Hunter L, Bogen J. 1996. Rates of erosion and sediment evacuation by glaciers: A review of field data and their implications. *Global and Planetary Change* 12:213–235.
- Hansen L. 2004. Deltaic infill of a deglaciated arctic fjord, East Greenland: Sedimentary facies and sequence stratigraphy. *Journal of Sedimentary Research* 74(3):422–437.
- Helland-Hansen W, Gjelberg JG. 1994. Conceptual basis and variability in sequence stratigraphy: A different perspective. *Sedimentary Geology* 92:31–52.
- Helle SK. 2004. Sequence stratigraphy in a marine moraine at the head of Hardangerfjorden, western Norway: Evidence for a high-frequency relative sea-level cycle. *Sedimentary Geology* 164:251–281.
- Hooke R LeB. 1976. Pleistocene ice at the base of the Barnes Ice Cap, Baffin Island, N.W.T., Canada. *Journal of Glaciology* 17:1174–1188.
- Hughen KA, Baillie MGL, Bard E, Bayliss A, Beck JW, Blackwell PG, Buck CE, Burr GS, Cutler KB, Damon PE, Edwards RL, Fairbanks RG, Friedrich M, Guilderson TP, Herring C, Kromer B, McCormac FG, Manning SW, Ramsey CB, Reimer PJ, Reimer RW, Remmele S, Southon JR, Stuiver M, Talamo S, Taylor FW, van der Plicht J, Weyhenmeyer CE. 2004. Marine04 Marine radiocarbon age calibration, 26–0 ka BP. *Radiocarbon* 46:1059–1086.
- Jacobs JD, Heron R, Luther JE. 1993. Recent changes at the Northwestern margin of the Barnes Ice Cap, Baffin Island, N.W.T. Canada. *Arctic and Alpine Research* 25(4):341–352.
- Janszen A, Moreau J, Moscariello A, Ehlers J, Krögers J. 2013. Time-transgressive tunnel-valley infill revealed by a three-dimensional sedimentary model, Hamburg, north-west Germany. *Sedimentology* 60:693–719.
- Kalefa El-ghali MA. 2005. Depositional environments and sequence stratigraphy of paralic glacial, paraglacial and postglacial Upper Ordovician siliciclastic deposits in the Murzuq Basin, SW Libya. *Sedimentary Geology* 177:145–173.
- Kaplan MR, Wolfe AP. 2006. Spatial and temporal variability of Holocene temperature in the North Atlantic Region. *Quaternary Research* 65:223–231.
- Koppes MN, Montgomery DR. 2009. The relative efficacy of fluvial and glacial erosion over modern to orogenic timescales. *Nature Geoscience* 2:644–647.
- Lambeck K, Chappell J. 2001. Sea level change through the last Glacial Cycle. *Science* 292:679–686.
- Le Heron DP, Craig J, Sutcliffe OE, Whittington R. 2006. Late Ordovician glaciogenic reservoir heterogeneity: An example from the Murzuq Basin, Libya. *Marine and Petroleum Geology* 23:655–677.
- Levell BK, Braakman JH, Rutten KW. 1988. Oil-bearing sediments of Gondwana Glaciation in Oman. *American Association of Petroleum Geologists Bulletin* 72(7):775–796.
- Løken OH. 1965. Postglacial emergence at the south end of Inugsuin Fiord, Baffin Island, N.W.T. *Geographic Bulletin* 7:243–258.
- McGregor K, Anderson RS, Anderson SP, Waddington ED. 2000. Numerical simulation of glacial-valley longitudinal profile evolution. *Geology* 28(11):1031–1034.
- Miller GH, Wolfe AP, Briner JP, Sauer PE, Nesje A. 2005. Holocene glaciation and climate evolution of Baffin Island, Arctic Canada. *Quaternary Science Reviews* 24:1703–1721.
- Miller GH, Wolfe AP, Steig EJ, Sauer PE, Kaplan MR, Briner JP. 2002. The Goldilocks dilemma: Big ice, little ice, or “just right” ice in the Eastern Canadian Arctic. *Quaternary Science Reviews* 21:33–48.
- Østrem G, Bridge CW, Rannie WF. 1967. Glacio-hydrology, discharge and sediment transport in the Decade Glacier Area, Baffin Island, N.W.T. *Geographiska Annaler* 49A:268–282.
- Overeem I, Bishop C, Weltje GJ, Kroonenberg SB. 2001. The Late Cenozoic Eridanos delta system in the Southern North Sea Basin: A climate signal in sediment supply? *Basin Research* 13(3):293–312.
- Overeem I, Syvitski JPM. 2010. Experimental exploration of the stratigraphy of fjords fed by glaciofluvial systems. In Howe J, Austin W, Forwick M, Paetzel M (Editors). *Fjords Systems and Archives*, Special Publication 344: Geological Society, London. p. 125–142.
- Overeem I, Syvitski JPM, Hutton EWH, Kettner AJ. 2005. Stratigraphic variability due to uncertainty in model boundary conditions: A case-study of the New Jersey Shelf over the last 40,000 years. *Marine Geology* 224:23–41.
- Peltier WR. 2004. Global glacial isostasy and the surface of the Ice-Age Earth: The ICE-5G Model and GRACE. *Annual Review Earth Planetary Science* 32:111–149.
- Powell RD, Cooper JM. 2002. A glacial sequence stratigraphic model for temperate, glaciated continental shelves. In Dowdeswell JA, Cofaigh CO (Editors). *Glacier Influenced Sedimentation on High-latitude Continental Margins*, Special Publication 203: Geological Society, London. p. 215–244.
- Powell RD, Elverhoi A. 1989. Modern glaciomarine environments: Glacial and marine controls of modern lithofacies and biofacies. *Marine Geology* 85:101–418.
- Prior DB, Bornhold BD, Wiseman WJ Jr, Lowe DR. 1987. Turbidity current activity in a British Columbia fjord. *Science* 237:1330–1333.
- Schack Pedersen S. 2012. Glaciodynamic sequence stratigraphy. In Huuse M, Redfern J, Le Heron DP, Dixon RJ, Moscariello A, Craig J (Editors). *Glaciogenic Reservoirs and Hydrocarbon Systems*, Special Publication 368: Geological Society, London. p. 29–51.
- Smith RW, Bianchi TS, Allison M, Savage C, Galy V. 2015. High rates of organic carbon burial in fjord sediments globally. *Nature Geoscience* 8:450–453.
- Storms J, de Winter I, Overeem I, Drijkoningen GG, Lyke-Andersen H. 2012. The Holocene sedimentary history of the Kangerlussuaq Fjord valley fill, West Greenland. *Quaternary Science Reviews* 35:29–50.
- Stravers JA, Syvitski JPM. 1991. Early Holocene land-sea correlations and deglacial evolution of the Cambridge Fiord basin, Northern Baffin Island. *Quaternary Research* 35:72–90.
- Stravers JA, Syvitski JPM, Praeg DB. 1991. Application of size sequence data to glacial-paraglacial sediment transport and sediment partitioning. In Syvitski JPM (Editor). *Principles, Methods and Application of Particle Size Analysis*: Cambridge University Press, New York. p. 293–310.
- Stuiver M, Reimer PJ, Reimer RW. 2005. CALIB 5.0. [www.calib.org/calib](http://www.calib.org/calib). Accessed March 3, 2017.
- Syvitski JPM (Editor). 1983. Sedimentology of Arctic Fjords Experiment: HU 83-028 Data report, Volume 2. Canadian Data Report of Hydrography and Ocean Sciences, No. 28. Bedford Institute of Oceanography, Canada.
- Syvitski JPM. 1991. Towards an understanding of sediment deposition on glaciated continental shelves. *Continental Shelf Research* 11(8–10):897–937.
- Syvitski JPM, Blakeney CP (Editors). 1983. Sedimentology of Arctic Fjords Experiment: HU 82-031 Data report, Volume 1. Canadian Data Report of Hydrography and Ocean Sciences, No. 12. Bedford Institute of Oceanography, Canada.
- Syvitski JPM, Burrell DC, Skei JM. 1987. *Fjords: Processes & Products*: Springer-Verlag, New York. 379 p.
- Syvitski JPM, Farrow GE, Atkinson RJA, Moore PG, Andrews JT. 1989. Baffin Island fjord macrobenthos: Bottom communities and environmental significance. *Arctic* 42:232–247.
- Syvitski JPM, Hein FJ. 1991. Sedimentology of an arctic basin: Itirbilung Fiord, Baffin Island, Canada. *Geological Survey of Canada Professional Paper* 91-11, 67 p.

- Syvitski JPM, Praeg DB (Editors). 1984. Sedimentology of Arctic Fjords Experiment: Data report, Volume 3. Canadian Data Report of Hydrography and Ocean Sciences, No 54. Bedford Institute of Oceanography, Canada.
- Thompson RS, Anderson KH, Bartlein PJ. 1999. *Atlas of Relations between Climatic Parameters and Distributions of Important Trees and Shrubs in North America*: US Geological Survey Professional Paper 1650-A and B.
- Van der Vegt P, Janszen A, Moscariello A. 2012. Tunnel Valleys: Current knowledge and future perspectives. In Huuse M, Redfern J, Le Heron DP, Dixon RJ, Moscariello A, Craig J (Editor). *Glaciogenic Reservoirs and Hydrocarbon Systems*, Special Publication 368: Geological Society, London. p. 75–97.
- Williams KM, Andrews JT, Jennings AE, Short SK, Mode WN, Syvitski JPM. 1995. The Eastern Canadian Arctic at 6 KA. *Géographie Physique et Quaternaire* 49:13–27.
- World Data Center for Marine Geology and Geophysics (WDC-MGG). 2000. International Bathymetric Chart of the Arctic Ocean. <http://www.ngdc.noaa.gov/mgg/bathymetry/arctic/arctic.html>. Accessed March 3, 2017.